

**US Department of Energy, Office of Science**  
**Office of Biological and Environmental Research (BER)**  
**Subsurface Biogeochemical Research (SBR)**  
**FY11 First Quarter Performance Measure**

## **Introduction**

This first quarter FY11 SBR overall Performance Assessment Rating Tool (PART) measure is focused on the topic: *Using Advanced Computational Models to Better Understand Multiscale Processes that affect Contaminant Transport at Field Scales*. This milestone is focused on research being performed at the Hanford Integrated Field Research Challenge (IFRC) site, located in the 300 Area at the Hanford Site in southeastern Washington State, in conjunction with a SciDAC-2 project to apply high performance computing to DOE contaminated sites. There are two major hurdles in modeling multiscale processes that must be overcome. One is the computational resources needed to solve the governing equations for multicomponent chemically reacting systems, and the other is determining site-specific model parameters derived from field observations. There are a number of different formulations of multiscale models including multiple interacting continua and multirate models which are discussed in some detail in what follows.

To investigate the causes and mechanisms behind the slow leaching of uranium observed at the Hanford 300 Area, an IFRC project was formed to study the mobility of uranium at the site. A primary hypothesis of the project was that multiscale processes were fundamental for understanding uranium mobility and its slow release from contaminated sediment. The 1600 m<sup>2</sup> Hanford IFRC site contains 36 groundwater monitoring wells placed within the footprint of the South Process Pond where uranium wastes were discharged. A 2 km<sup>2</sup> U(VI) groundwater plume exists at this location that exceeds regulatory limits and has persisted over time despite efforts to remediate the site. Original predictions by Westinghouse Hanford in the early 1990s indicated that the plume would dissipate in 3–10 years. Obviously this prediction has not come to pass. The Westinghouse model was based on a constant  $K_d$  assumption which, for a number of reasons discussed below, is inadequate for this site.

A recent 3D modeling study by Hammond and Lichtner (2010) using the computer code PFLOTRAN, a DOE SciDAC-2 funded massively-parallel, multiphase, reactive flow and multi-component transport code, was the first to attempt to predict the discharge rate of uranium into the Columbia River. The results were in good agreement with field estimates with a value on the order of 50 kg/y (Peterson et al., 2009). The model also correctly predicted the discharge rate of groundwater to the river estimated at  $2 \times 10^9$  kg/y. Interestingly, the model calculations by Hammond and Lichtner (2010) showed that sorption played only a secondary role in de-

terminating the flux of uranium to the Columbia River. This is essentially because of the finite path length (~100 m) the uranium must travel to reach the river. During the migration of the uranium front the sorption sites between the source region and the river become equilibrated with uranium and retardation is minimal after the front reaches the discharge point. This observation is expected to apply to other contaminated sites as well provided the discharge point is close enough to the source region. From mass balance considerations, the authors noted that the leach rate of uranium from the source region must balance the discharge into the river. Knowing the average leaching rate and mean discharge to the river would thus enable the total volume of contaminated sediment to be estimated. DOE is actively evaluating suitable and effective remedial strategies for the site and it is hoped that the information provided in this report will be valuable in aiding this effort.

## **Different Flavors of Multiscale/Multirate Models**

A fundamental problem facing efforts to model subsurface reactive flows is characterizing and incorporating a multitude of spatial scales that are typical of natural systems into multicomponent-multiphase numerical models. Spatial scales may range from nanoscale surface chemistry, to pore and fracture apertures of millimeters to centimeters, to fracture spacing and matrix block sizes of tens of centimeters to meters, to reservoir or basin scales of kilometers to tens of kilometers. To illustrate the technical challenges involved in modeling multi-scale subsurface processes, consider a basin scale reservoir with an areal extent of one square kilometer and depth of 500 meters. Modeling this system as a single continuum on a grid with one million nodes results in an average grid block size of 10m by 10m by 5m—or roughly the size of a large conference room. Within this grid block, physical and chemical processes occur at much smaller sub-grid scales. Such processes involve, for example, diffusive and advective mass transfer between fractures and rock matrix, or more generally diffusion between macro- and micro-pore scales, accompanied by chemical reactions. Characteristic of these systems is mass transport and chemical reactions occurring at disparate spatial scales that cannot be captured within a single continuum description. In particular, localized chemical environments may be vastly different from the bulk fluid and lead to dramatically different results compared to a single continuum description. It is clearly impossible to capture this range of scales within a single continuum framework because of the large computational expense that would be required to resolve the smallest scale. One approach that appears feasible to describe such systems is to incorporate sub-grid scale processes through multiple interacting continua representing fine scale processes. Besides the difficulty developing conceptual models of such systems, characterization at the laboratory and field scales adds additional challenges. In addition, this approach carries a significant computational cost as well because of the increase in the number of degrees of freedom associated with the additional continua and the necessity to carry out calculations over engineering and geologic time spans within feasible computation times.

Multiscale processes range from millimeter scales or smaller to macroscales of tens of meters or larger (see Figure 1). Capturing this extreme range of scales is impossible with current and near-future computing capabilities employing conventional single continuum models with simple orthogonal grids. For example, discretizing a computational domain measuring  $2 \text{ km} \times 1 \text{ km} \times 500 \text{ m} = 10^9 \text{ m}^3$ , into cubic millimeter nodes would require  $10^{18}$  computational nodes to describe. Reducing the grid spacing by just a factor of 10 in each dimension of a 3D domain, increases the number of nodes by a factor of 1000. Clearly alternative approaches are needed for capturing small-scale processes at the field scale. Two promising possibilities to resolve this problem are to apply grid refinement only where needed using adaptive mesh refinement (AMR) techniques, and incorporate a sub-grid scale model that can account for millimeter scales into the primary-grid continuum model. This latter approach is commonly used to describe fractured porous media based on a dual continuum representation as a special case of a sub-grid model, but the concept applies more generally to multiscale media represented by multiple interacting continua.

Multicomponent lattice Boltzmann simulations at the pore scale conducted with synthetic pore geometries indicate that to accurately represent breakthrough curves for the effluent concentration, a dual continuum model is generally required (Lichtner and Kang, 2007). In this formulation, one continuum represents the bulk fluid (primary continuum), and the other continuum (matrix or secondary continuum) represents dead-end pores and secondary porosity that is connected by diffusive (or advective) transport to the primary continuum. Dual (and more generally multiple) continuum formulations appear adequate for sufficiently slow reaction rates where concentration gradients within a single pore do not exist. As the rate increases to larger values where concentration gradients within a single pore are present, continuum formulations may fail, and hybrid approaches are needed which account for different physics on different scales. A classic example of this situation is the formation of wormholes during acidization processes. Wormholes result from reaction instabilities responding to pore scale heterogeneities and require pore scale simulations where Darcy's law no longer holds.

Several different approaches have been or are currently being implemented in PFLOTRAN to describe multiscale processes. These approaches include a mobile-immobile domain model, a multiple interacting continua approach, and a multirate model. Of these, the multirate sorption model is the least computationally intensive using the numerical implementation detailed in Hammond and Lichtner (2010). The multiple interacting continua model has the greatest computational burden, while the mobile-immobile formulation only doubles the number of degrees of freedom compared to a single continuum model.

## Multiple Continuum Model

There are several different formulations of multiscale continuum models which may be distinguished by the connectivity of the primary and secondary continua (Lichtner, 2000). These are referred to as the DCCM (dual continuum connected matrix) and DCDM (dual continuum disconnected matrix models). Here the term primary continuum refers to the continuum in which bulk fluid flow takes place and is usually represented as a 3D connected domain. It may, for example, refer to a fracture network represented as a porous medium or the macro-pores in a soil. Secondary, or sub-grid scale continua are coupled locally to the primary continuum. Often only diffusion is allowed in the sub-grid continua which are represented by an effective 1D geometry, although flow is also possible in principal.

Distinguishing between different domains is somewhat arbitrary and nonunique (Lichtner and Kang, 2007). Which pores participate in flow depends on the degree of saturation of the medium. A typical approach is to divide pores into macro pores which carry the bulk fluid and micro pores which are connected to macro pores by diffusion. Inter- (between macro pores) and intra- (inside micro pores) mass transfer between the different pores is formulated as a set of coupled partial differential equations based on the generalization of a single continuum to several interacting continua. One of the primary difficulties in applying a multiscale formulation is obtaining values for the parameters that enter into the model. As has been demonstrated for a linear single component system these values may be nonunique (Sardin et al., 1991).

It can be demonstrated that the multirate model is equivalent to a multiple continuum formulation under very special conditions of a single component with a linear  $K_d$  approximation. This was shown for a two-site sorption model and mobile-immobile domain by Nkedi-Kizza et al. (1984). This result can be easily generalized to multi-site sorption and multi-domain models for linear systems. Multiscale processes play a significant role in many situations involving flow and reactive transport. However, because of the inherent nonlinearity of constitutive relations, for example, chemical rate laws and statements of equilibrium mass action relations in real multicomponent fluids, use of linear relations is of limited usefulness.

In the following a multi-scale continuum formulation for reactive transport is developed based on multiple interacting continua. In this formulation the primary continuum, which may consist of one, two, or three spatial dimensions, is coupled to sub-grid scale domains that are presumed to form effective one-dimensional regions (see Figure 2) with simple geometries of sphere, cubes or cylinders. In this model, the sub-grid domains are coupled only to the primary continuum and not to each other as illustrated in Figure 2 which shows the connectivity between primary and secondary continua. The algorithm presented below provides for local concentration gradients within a sub-continuum domain and places no restrictions on linear or nonlinear constitutive relations. It is completely general in the treatment of chemical and other physical processes.

Multi-scale, multicomponent, Darcy continuum-scale reactive transport equations for primary species  $\mathcal{A}_j$  participating in aqueous complexing, mineral precipitation/dissolution and surface complexation reactions can be written in the general form as the set of coupled partial differential equations as follows (Lichtner and Kang, 2007)

$$\frac{\partial}{\partial t} \left( \epsilon_\alpha \varphi_\alpha \Psi_j^\alpha + \sum_l \nu_{jl} S_l^\alpha \right) + \nabla \cdot \mathbf{\Omega}_j^\alpha = \sum_\beta a_{\alpha\beta} \Omega_j^{\alpha\beta} - \epsilon_\alpha \sum_s \nu_{js} I_s^\alpha, \quad (1)$$

for the primary continuum fluid, and

$$\frac{\partial}{\partial t} \left( \varphi_\beta \Psi_j^\beta + \sum_l \nu_{jl} S_l^\beta \right) + \nabla \cdot \mathbf{\Omega}_j^\beta = - \sum_s \nu_{js} I_s^\beta, \quad (2)$$

for the  $\beta$ th sub-grid domain, with total concentration  $\Psi_j^{\alpha,\beta}$  and flux  $\mathbf{\Omega}_j^{\alpha,\beta}$ . The quantity  $\epsilon_\alpha$  represents the volume fraction occupied by the primary continuum. The volume averaged kinetic mineral reaction rate  $I_s^{\alpha,\beta}$  has the form

$$I_s^{\alpha,\beta} = -k_s^{\alpha,\beta} a_s^{\alpha,\beta} (1 - K_s Q_s^{\alpha,\beta}), \quad (3)$$

with rate constant  $k_s^{\alpha,\beta}$  and mineral surface area  $a_s^{\alpha,\beta}$  for primary continuum  $\alpha$  and sub-grid continua  $\beta$ . The total solute flux includes advective and diffusive terms

$$\mathbf{\Omega}_j^{\alpha,\beta} = -\epsilon_{\alpha,\beta} \varphi_{\alpha,\beta} \tau_{\alpha,\beta} D \nabla \Psi_j^{\alpha,\beta} + \mathbf{q}_{\alpha,\beta} \Psi_j^{\alpha,\beta}, \quad (4)$$

with tortuosity  $\tau_{\alpha,\beta}$ , diffusivity  $D$  in the absence of a solid phase, and Darcy flow rate  $\mathbf{q}_{\alpha,\beta}$ . For simplicity the dispersion tensor is not included, but in general would be necessary in a Darcy continuum description. The sorption isotherm is denoted by  $S_l^{\alpha,\beta}$ .

The boundary condition at the primary continuum- $\beta$ -secondary continua fluid interface is given by

$$C_j^\beta(r = r_\beta, t; \mathbf{r}) = C_j^\alpha(\mathbf{r}, t), \quad (5)$$

where  $r_\beta$  denotes the boundary of the domain  $\beta$ . The flux at the primary continuum-matrix interface is presumed to only involve diffusion with the form

$$\Omega_j^{\alpha\beta} = -\varphi_\beta \tau_\beta D \mathbf{n}_\beta \cdot \nabla \Psi_j^\beta \Big|_{r_\beta}, \quad (6)$$

where  $\mathbf{n}_\beta$  denotes the outward normal to the interface. The matrix equation is quite general and applies to various geometries including spheres and linear domains. As an approximation cubes and irregular shaped domains may be used. Because of computational considerations, the sub-grid domain equations are reduced to an equivalent 1D problem. For further discussion of numerical techniques for efficiently solving the multi-scale equations see Lichtner (2000).

## Multirate Model

Another approach to modeling multiscale processes is the multirate sorption model developed by Liu et al. (2008). In this model a spectrum of rate constants are introduced to describe complex sorption processes that may take place both in primary and secondary pores, the latter being connected to the primary continuum through diffusive pathways. The multirate model has a distinct advantage compared to multiscale continuum models in that it does not result in an increase in the number of degrees of freedom (Hammond and Lichtner, 2010). The distribution of rate constants are determined through a probability distribution function such as a log-normal distribution. Thus the rate constants may be parameterized by the two quantities, the mean and variance, that characterize the probability distribution. In addition, however, the rate constants also depend on the fraction of the site density assigned to each rate. Usually this is taken as a single uniform value for all rate constants which leads to some ambiguity in the physical interpretation of the multirate model (Hammond and Lichtner, 2010). Multicontinuum models have also been applied to the Hanford site [see Figure 3, Lichtner (unpublished)] with some success, but generally the fits using a single secondary continuum are not as good as the multirate model. Presumably using several secondary continua would improve the fit.

The multirate solute transport equations have the form

$$\frac{\partial}{\partial t} \varphi \Psi_j + \nabla \cdot \mathbf{\Omega}_j = - \sum_{i\alpha} v_{ji} \frac{\partial S_{i\alpha}}{\partial t} - \sum_m v_{jm} I_m, \quad (7a)$$

or

$$\frac{\partial}{\partial t} \left( \varphi \Psi_j + \sum_{i\alpha} v_{ji} S_{i\alpha} \right) + \nabla \cdot \mathbf{\Omega}_j = - \sum_m v_{jm} I_m, \quad (7b)$$

where in the latter form the sorption isotherm has been moved to the left-hand side of the equation. In terms of the locally defined distribution coefficient  $K_j^d$  this latter equation can be written in the form

$$\frac{\partial}{\partial t} \left[ \varphi \Psi_j (1 + K_j^d) \right] + \nabla \cdot \mathbf{\Omega}_j = - \sum_m v_{jm} I_m, \quad (8)$$

where

$$K_j^d = \frac{1}{\varphi \Psi_j} \sum_{i\alpha} v_{ji} S_{i\alpha}. \quad (9)$$

When the distribution coefficient is constant, the transport equation can be expressed in terms of retarded transport coefficients and mineral reaction rate constants

$$\frac{\partial}{\partial t} (\varphi \Psi_j) + \nabla \cdot \frac{1}{\mathfrak{R}_j} \mathbf{\Omega}_j = - \frac{1}{\mathfrak{R}_j} \sum_m v_{jm} I_m, \quad (10)$$

where

$$\mathfrak{R}_j = 1 + K_j^d. \quad (11)$$

In the multirate model the rates of sorption reactions are described through a kinetic relation given by

$$\frac{\partial S_{i\alpha}}{\partial t} = k_{\alpha}(S_{i\alpha}^{\text{eq}} - S_{i\alpha}), \quad (12)$$

for the  $i$ th surface complex on site  $\alpha$ . With each site  $\alpha$  is associated a rate constant  $k_{\alpha}$  and site concentration  $\omega_{\alpha}$ . These quantities are defined through a given distribution of sites  $\wp(\alpha)$ , such that

$$\int_0^{\infty} \wp(k_{\alpha}) dk_{\alpha} = 1. \quad (13)$$

The fraction of sites  $f_{\alpha}$  belonging to site  $\alpha$  is determined from the relation

$$f_{\alpha} = \int_{k_{\alpha}-\Delta k_{\alpha}/2}^{k_{\alpha}+\Delta k_{\alpha}/2} \wp(k_{\alpha}) dk_{\alpha} \approx \wp(k_{\alpha}) \Delta k_{\alpha}, \quad (14)$$

with the property that

$$\sum_{\alpha} f_{\alpha} = 1. \quad (15)$$

Given that the total site concentration is  $\omega$ , then the site concentration  $\omega_{\alpha}$  associated with site  $\alpha$  is equal to

$$\omega_{\alpha} = f_{\alpha} \omega. \quad (16)$$

## High Performance Computing (HPC) and Numerical Implementation of Multiscale Continuum Models

The use of multiscale continuum models in field-scale simulations has been severely limited by the lack of parallel implementations employing HPC. These models at best double the number of degrees of freedom in the DCCM formulation and lead to potentially orders of magnitude or more in the number of degrees of freedom compared to a single continuum in the DCDM approach.

Incorporating sub-grid scale processes in a field scale 3D domain involves a considerable computational investment. In the DCDM multiple continuum model, to reduce the computational resources the sub-grid model is represented as an effective 1D domain, corresponding for example to spheres, cubes, or other geometries. Multiple sub-grid models may be associated with a subset of nodes in the primary continuum. These different sub-grid models correspond to rock fragments of different sizes and mineral compositions. Thus the incorporation of a sub-grid model in a multicomponent system increases the number of degrees of freedom from order  $N^D$ , where  $N$  represents the number of nodes in a single spatial dimension for the primary continuum grid, and  $D$  denotes the number of spatial dimensions, to  $N^D \times N_K \times N_{\text{DCM}} \times N_C$ , where  $N_K$  denotes the number of different sub-grid classes,  $N_{\text{DCM}}$  refers to the number of nodes used to discretize the subdomain, and  $N_C$  refers to the number of primary chemical species. Thus

incorporation of a sub-grid scale model can increase the array size of the concentration field variable by several orders of magnitude. It should be noted, however, that because the sub-grid continua act as a source or sink term to the 3D primary continuum, it is not necessary to include a sub-grid model at every primary continuum node. This could greatly reduce the computational complexity.

Fortunately, this system of equations can be broken up into two subsets corresponding to the 3D primary continuum equations and the secondary continua equations. The primary continuum equations may be solved using the usual domain decomposition approach for parallelization with parallel Newton-Krylov solvers such as provided in the PETSc parallel framework. The equations for the secondary continua are embarrassingly parallel and consequently should be well-suited for implementation on heterogeneous architectures employing GPU processors. The DCDM formulation is currently being implemented in PFLOTRAN (Kumar et al., 2010).

## **Multiscale Contaminant Transport at the Field-Scale: the Hanford 300 Area**

### **Hanford 300 Area**

Recently, Hammond and Lichtner (2010) carried out an extensive 3D study of the Hanford 300 Area using HPC. The model domain used is the simulations measured  $900 \text{ m} \times 1300 \text{ m} \times 20 \text{ m}$  with a grid resolution of  $\Delta x = \Delta y = 5 \text{ m}$ ,  $\Delta z = 0.5 \text{ m}$  using  $180 \times 260 \times 40$  cells, and with 15 chemical components leading to over 28 million degrees of freedom. Calculations were carried out on Jaguar, a Cray XT5 machine at ORNL, using 4096 processor cores. This was the first simulation of the U(VI) plume at the 300 Area which included the effects of fluctuations in the Columbia River stage, the role of the hyporheic zone on groundwater velocities, and a vadose zone U(VI) source term to replenish the plume. Sorption was included in the model calculations through both equilibrium and multirate models, the latter determined to be essential in describing U(VI) breakthrough curves in column leaching experiments (Liu et al., 2008). The results obtained were in good agreement with field estimates for the flux of U(VI) of 50 kg/y and water of  $2 \times 10^9 \text{ kg/y}$  (Peterson et al., 2009). Perhaps the most surprising result of the simulations, however, was the discovery that sorption played only a minor role in determining the cumulative flux of U(VI) into the Columbia River [see Figure 4, reproduced from Hammond and Lichtner (2010)]. Results for the cumulative U(VI) flux to the river for no sorption and equilibrium and multirate sorption models were all essentially the same. Until this study, it had been generally thought that multiscale processes involving sorption were to blame in determining the longevity of the uranium plume at the site.



An explanation of the lack of sensitivity of the rate of discharge of uranium into the Columbia River on sorption can be understood by realizing that once sorption sites are equilibrated with a sorbing contaminant, the contaminant can move freely unretarded to the discharge point. Mixing of groundwater and river water will perturb this equilibrium state, leading to stabilization of the plume; however, the mean flux to the river is not substantially affected. By mass balance under pseudo-steady state conditions, it is clear that the release rate of the contaminant from the source region is related to its rate of discharge into the river.

The large fluctuations, on the order of meters, in the Columbia River stage causing water table levels to rise and fall has a number of effects on the mobility of uranium. For example, this can result in the release and potentially redeposition of contaminants higher up in the vadose zone. Hammond and Lichtner (2010) found that dissolution as well as reprecipitation of uranium may occur causing it to be recycled between aqueous and solid phases. In addition, river stage fluctuations lead to large fluctuations in the flow velocity, both in direction and magnitude.

One needs to ask at this point, what level of detail is really needed to understand uranium migration at the 300 Area site. A common sense approach generally holds that in order to understand reactive transport one must first understand the details of the flow field and the behavior of a non-reactive tracer. This maxim, however, may not necessarily be true at the 300 Area depending on what process or processes one is attempting to understand. The movement of a tracer at the 300 Area is highly complicated and depends on many details such as the heterogeneity of the sediment, river stage fluctuations and capillary properties of the vadose zone. However, if one is only interested in the cumulative flux of uranium into the Columbia River for the purpose of studying natural attenuation of uranium at the site, then all this detail may not be so interesting or needed. For example, Hammond et al. (2010a) found that heterogeneity had little if any effect on the cumulative flux of uranium into the Columbia River, whereas the flow velocity was highly sensitive from one realization to another.

Another case in point is the somewhat paradoxical interpretation of the Liu et al. (2008) stop-flow column experiments which clearly require a multirate model to fit the U(VI) breakthrough curve unlike the field situation (Hammond and Lichtner, 2010). However, once one realizes that the leaching conditions of the experiment are very different from field conditions where sorption sites remain on average equilibrated with U(VI), it becomes clear that this experiment does not actually represent the field situation. This shows that behavior in the field can be drastically different compared to behavior in the laboratory even for the same sediment properties because of different boundary conditions, for example. It also shows the difficulty in identifying the relevant processes and attributing them to multiscale effects.

One essential parameter would appear to be the average leach rate of the contaminant from the source region which one might expect to be controlled at least partially by multiscale effects. It should also be noted that the leach rate may be very small because of the large volume

of contaminated sediment. Determining the net leach rate of uranium from the Hanford sediment and what processes, physical and chemical, affect the leach rate remains an outstanding issue at the Hanford 300 Area. The leach rate is balanced through mass conservation by discharge of uranium into the Columbia River, estimated to be roughly 50 kg/y (Peterson et al., 2009; Hammond and Lichtner, 2010). Thus, for example, knowing the leach rate and the discharge to the river, would enable the volume of contaminated sediment to be estimated. Hammond and Lichtner (2010) used a leach rate of  $2 \times 10^{-11}$  mol/m<sup>3</sup>/s for the surrogate uranium-copper-bearing mineral metatorbernite. The rate was obtained by approximately fitting the maximum observed uranium concentration at the 300 Area. The contaminated sediment volume  $\mathcal{V}$  can be estimated from the expression

$$\mathcal{V} = \frac{\mathcal{D}}{\mathcal{R}}, \quad (17)$$

where  $\mathcal{D}$  represents the discharge of uranium into the Columbia River taken as 50 kg/y, and  $\mathcal{R}$  denotes the mean leach rate, yielding the value  $\mathcal{V} \approx 333,086$  m<sup>3</sup>, or an equivalent square footprint of 258 m on a side assuming a depth of 5 m.

The leach rate is expected to be described by multiscale processes involving both sorption and mineral precipitation and dissolution. Within the vadose zone the leach rate is expected to vary with depth as the watertable rises and falls. Recycling of uranium may occur through sorption/desorption and dissolution/precipitation reactions. Although details of the leach rate certainly depend on the form of uranium in the vadose zone, it may be possible to determine the net leach rate averaged over time without the necessity of knowing the precise details of the processes involved.

## Implications for other Contaminated DOE Sites

Applying multiscale/multirate models to field sites is complicated by the difficulty in obtaining data necessary to populate the model as well as in distinguishing multiscale effects from macroscale processes. A typical example of a contaminated site is the emplacement of waste within the vadose zone which then migrates to a discharge point, usually a river or stream (creek), some distance away from the source. Because the travel path length of the contaminant is finite, measured on the order of hundreds of meters, the contaminant could have sufficient time since its emplacement to travel the complete distance to the discharge point. Typical time scales range from 30 to 65 years since the beginning of the nuclear age in 1943. Once this has happened, however, sorptive processes no longer play a significant role in determining the migration rate of the contaminant and it moves essentially unretarded. This is because the sorption sites along the pathway have become equilibrated with the contaminant and are no longer effective in retardation. Such a process is thought to be in effect at the Hanford 300 Area, for example, as well as other DOE contaminated sites such as the F-Area Basin at Savannah River

Site and the Oak Ridge site. The addition of various amendments to control the plume can be expected to perturb this equilibrium relation causing sorption to again become significant.

## Multiscale Processes and the IFRC Site-Scale Plume Experiment

The IFRC site is a triangular well field 60 m on a side located at the South Process Pond at the Hanford 300 Area approximately 250 m from the Columbia River (see Figure 5). The wells have an average spacing of 10 m. The mean depth to the watertable is approximately 10 m, varying with the rise and fall of the Columbia River stage of several meters. The groundwater travel time across the well field is on the order of a few days and fluctuates in direction and magnitude caused by fluctuations in the river stage. Various injection experiments are planned at the site to investigate the mobility of U(VI). The calculations described below are an initial attempt to obtain information on the sensitivity of boundary conditions and model parameters in describing the injection experiments with the goal of applying more refined models in the future and identify multiscale processes that are operable at the site.

The IFRC October 2009 U(IV) desorption experiment setup involved an injection rate at well 2-9 of 180 gpm, for a duration: 6.5 hrs. Injected concentrations of U(VI) equal to 5 mg/L and Br<sup>-</sup> with 180 mg/L were used. A major complication at the site is the extremely dynamic flow regime with vertical flow occurring in fully-screened wells. This results in oscillatory U(VI) concentrations as a result of vertical flow in the wellbore as the river undulates up and down. In addition, the plume may leave the boundary of the site as river water intrudes and recedes.

Calculations were carried out using using the multiple realization capability of PFLOTTRAN (Hammond et al., 2010b). The code has the capability to run 100s to 1000s of realizations executed simultaneously on 100s to 1000s of processor cores within a single parallel job. Parallel simulations were executed on the Jaguar supercomputer at ORNL. A total of 64,000 processor cores were employed per ensemble of 500 realizations using 128 cores per realization. This results in 50,625 degrees of freedom per processor core for each realization. Note that each ensemble would require ~7 years to run on a desktop computer assuming parallel runs are 50% efficient. Running in parallel it takes only 2 hours to complete an ensemble of runs—the time to complete one realization.

A computational domain of  $120 \times 120 \times 15 \text{ m}^3$  was used in the simulations with a grid resolution of  $1 \times 1 \times 0.5 \text{ m}^3$  resulting in 430,000 grid cells. Geochemistry was represented by 15 primary and 88 secondary aqueous species, 2 minerals and 2 surface complexes. This resulted in a total of 6.48 million degrees of freedom per realization.

In performing the sensitivity calculations based on multiple realization simulations several different scenarios were considered:

- Multirate kinetic vs. equilibrium surface complexation
- Three boundary conditions: A, B, C (see triangles on map in Figure 5)
- U(VI) mineral dissolution vs. no dissolution

Each scenario consisting of 500 realizations required two hours to run on 64,000 processor cores.

Observations from this study include:

- Boundary condition A, Multirate, No Mineral and boundary condition C, Equilibrium, No Mineral delivered best overall fits based on visual inspection.
- Mineral dissolution results in overshoot of observed U(VI) concentrations, but could be reduced using a lower dissolution rate.
- Rate constants should be calibrated [lowered from  $2 \times 10^{-17}$  mol/cm<sup>3</sup>/sec used in Hammond and Lichtner (2010)].
- Equilibrium surface complexation almost always undershoots observed U(VI) concentrations.
- The three boundary conditions give significantly different results (compare A vs. B vs. C; see Figures 7, 8 and 9).

Future directions in this ongoing work include: Integrating updated field characterization results to generate random fields; calibrating multirate model parameters; quantifying non-labile (nonsorbing) U(VI) source terms; and implementing an adaptive mesh refinement algorithm to enable moving the boundary conditions imposed on the site to the river and farther inland.

## Path Forward

Future work at the IFRC site will involve using the structured adaptive mesh refinement (SAMR) capability of PFLOTRAN applied to the IFRC site. Through the SAMR capability it will be possible to embed a refined grid surrounding the IFRC site while maintaining boundary conditions at the Columbia River and at 900 m inland, far removed from the site itself. By using four to five levels of grid refinement for a domain surrounding the IFRC site compared to the coarse grid used in the plume-scale model (5 meters for  $\Delta x$  and  $\Delta y$ ), high resolution can be maintained at the site. This would give the finest level grid spacing of 0.3125 to 0.15625 meters which should

be quite sufficient. It would then be possible to model an injection experiment at the IFRC site using boundary conditions imposed at the river and inland corresponding to the plume-scale model. This would be the first such calculation of its kind. Finally, the multiple interacting continuum approach to representing multiscale processes will be investigated and compared with the mutirate approach.

## Authors

Authors of this report are Peter C. Lichtner (LANL, lichtner@lanl.gov) and Glenn E. Hammond (PNNL, glenn.hammond@pnl.gov).

*Acknowledgements:* DOE Office of Science OBER Subsurface Biogeochemical Research Program, Scientific Discovery through Advanced Computing (SciDAC-2) program, and DOE Office of Science INCITE Program (Supercomputing): 3 million hours on Oak Ridge National Laboratory's Jaguar supercomputer were consumed for this work.

## References

- Hammond, G.E. and Lichtner, P.C. (2010) Field-Scale Model for the Natural Attenuation of Uranium at the Hanford 300 Area using High Performance Computing, *Wat. Res. Res.* 46, W09527, doi:10.1029/2009WR008819, 1–31.
- Hammond, G.E., Lichtner, P.C., and Rockhold, M.L. (2010a) Stochastic Simulation of Uranium Migration at the Hanford 300 Area, JCH, in press.
- Hammond, G.E., X. Chen, P.C. Lichtner (2010b) Uncertainty Quantification for Uranium Migration at the Hanford 300 Area, AGU, San Francisco.
- Kumar, J., R.T. Mills, P.C. Lichtner, and G.E. Hammond (2010) Massively parallel multiple interacting continua formulation for modeling flow in fractured porous media using the subsurface reactive flow and transport code PFLOTRAN, AGU, San Francisco.
- Lichtner, P.C. and Q. Kang (2007) Upscaling Pore-Scale Reactive Transport Equations using a Multi-Scale Continuum Formulation, *43(12)*, W12S15, doi:10.1029/2006WR005664, 1–19.
- Lichtner, P. C., (2000) Critique of dual continuum formulations of multicomponent reactive transport in fractured porous media, *Dynamics of fluids in fractured rocks*. Geophysical Monograph 122.

- Liu, C., Zachara, J. M., Qafoku, N. P., Wang, Z. (2008), Scale-dependent desorption of uranium from contaminated subsurface sediments, *Water Resources Research*, Vol. 44, doi:10.1029/2007WR006478, 1–13.
- Nkedi-Kizza, P., J.W. Biggar, H.M. Selim, M. Th. van Genuchten, P.J. Wierenga, J.M. Davidson and D.R. Nielsen (1984) On the equivalence of two conceptual models for describing ion exchange during transport through an aggregated oxisol, *Water Resources Research*, 20, 1123–1130.
- Peterson, R.E., C.F. Brown, and R.J. Serne (2009) Mass Balance Aspects of Persistent Uranium Contamination in the Subsurface at the Hanford Site, Washington, PNNL-SA-67979, October 2009, Pacific Northwest National Laboratory, Richland, WA.
- Sardin M., D. Schweich, F.J. Leu, and M.Th. van Genchten (1991) Modeling the nonequilibrium transport of linearly interacting solutes in porous media: A review, *Wat. Res. Res.* 27, 2287–2307.

## Figures

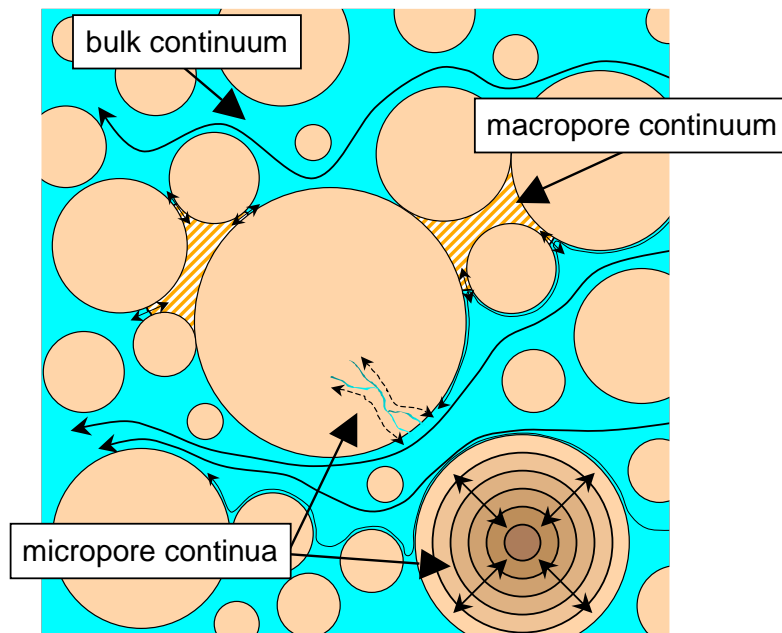


Figure 1: Schematic of a multiple continuum porous medium illustrating macro and micro pores with bulk flow and diffusion pathways.

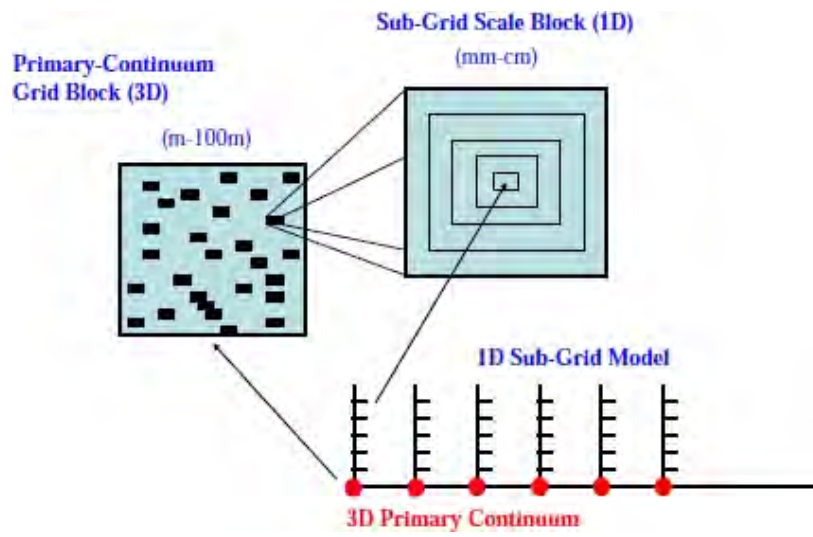


Figure 2: Structure of multiple continuum formulation.

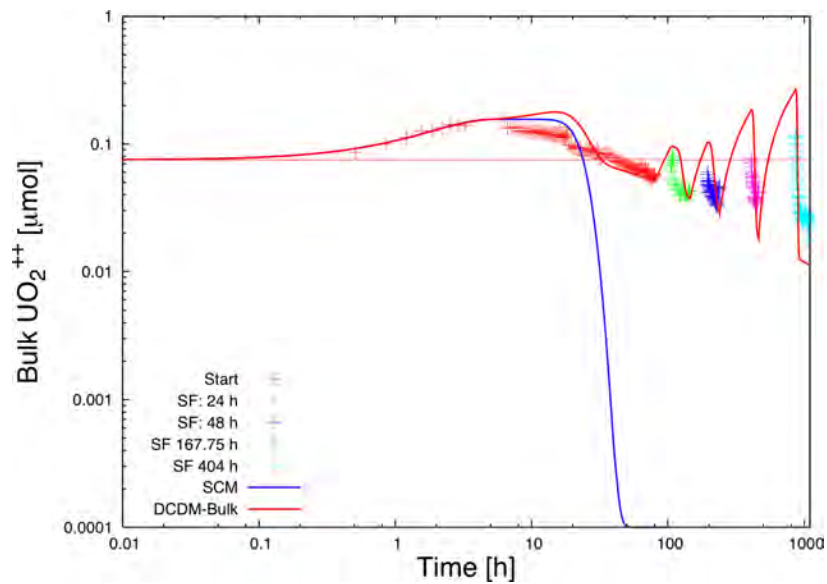


Figure 3: Fit to small column experiment using a dual continuum model formulation based on the DCDM approach.



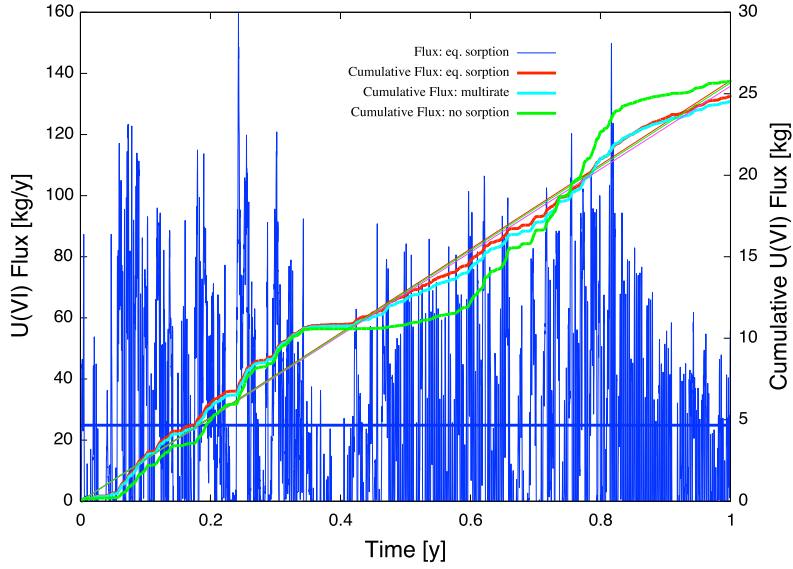


Figure 4: Calculated instantaneous and mean flux of U(VI) into the Columbia River plotted as a function of time (Hammond and Lichtner, 2010).

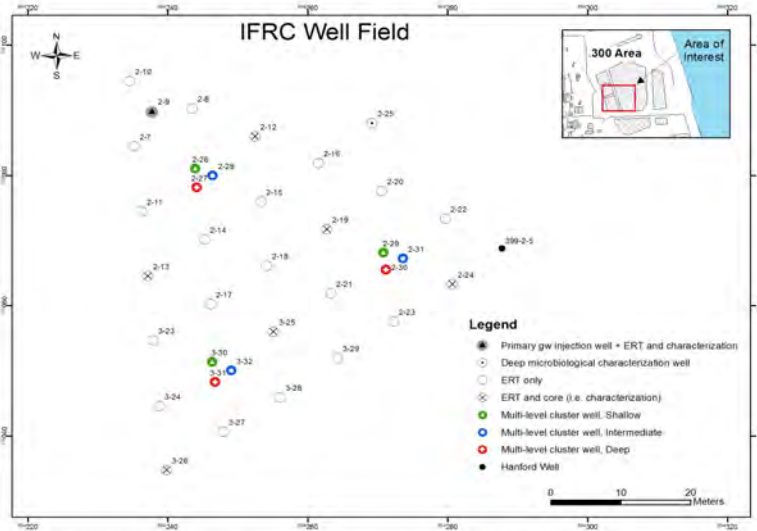


Figure 5: IFRC well field.



Figure 6: Boundary conditions for scenarios A (green), B (red) and C (black).

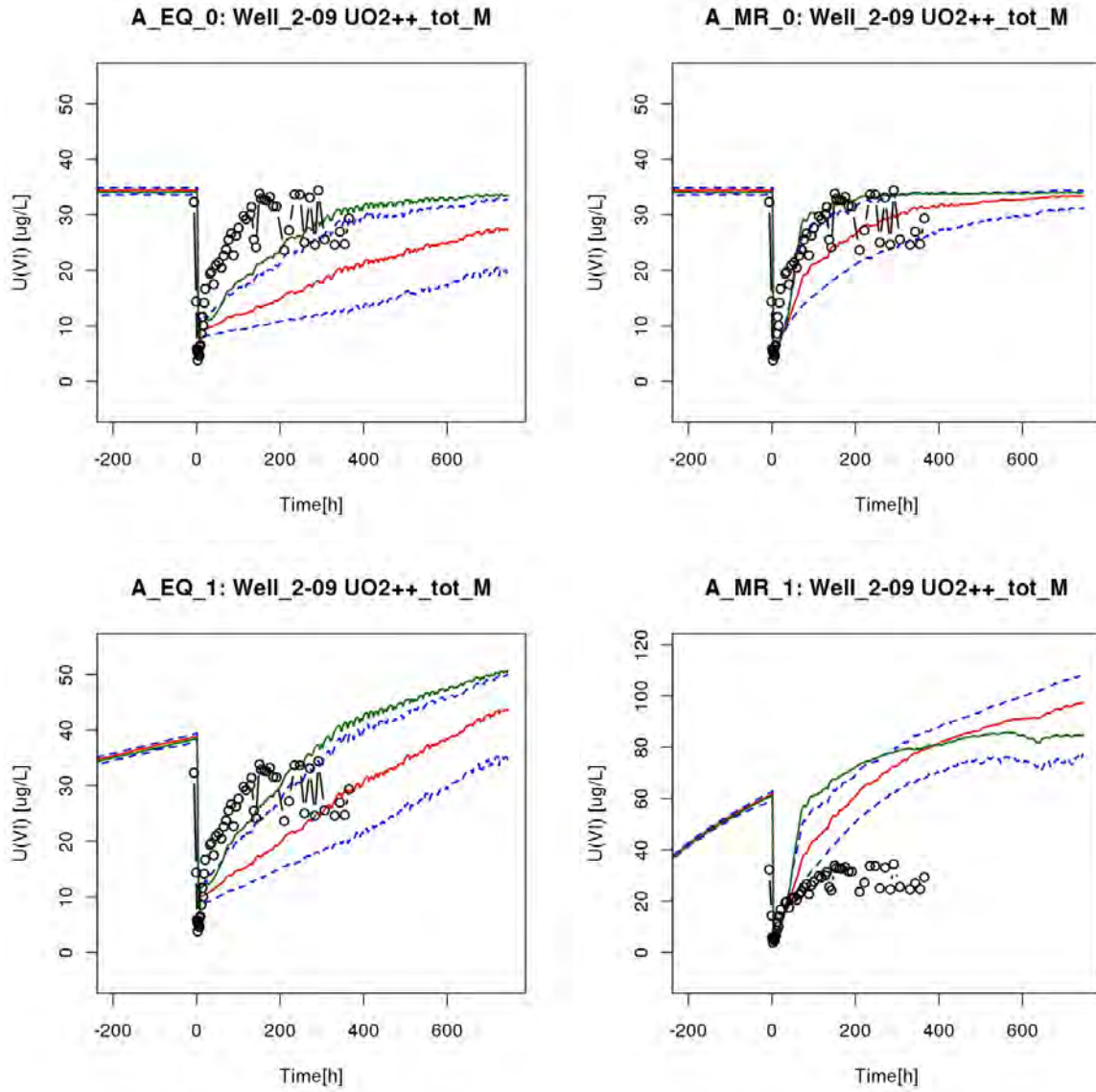


Figure 7: Comparison of model simulations for U(VI) concentration with field data for boundary condition scenario A.

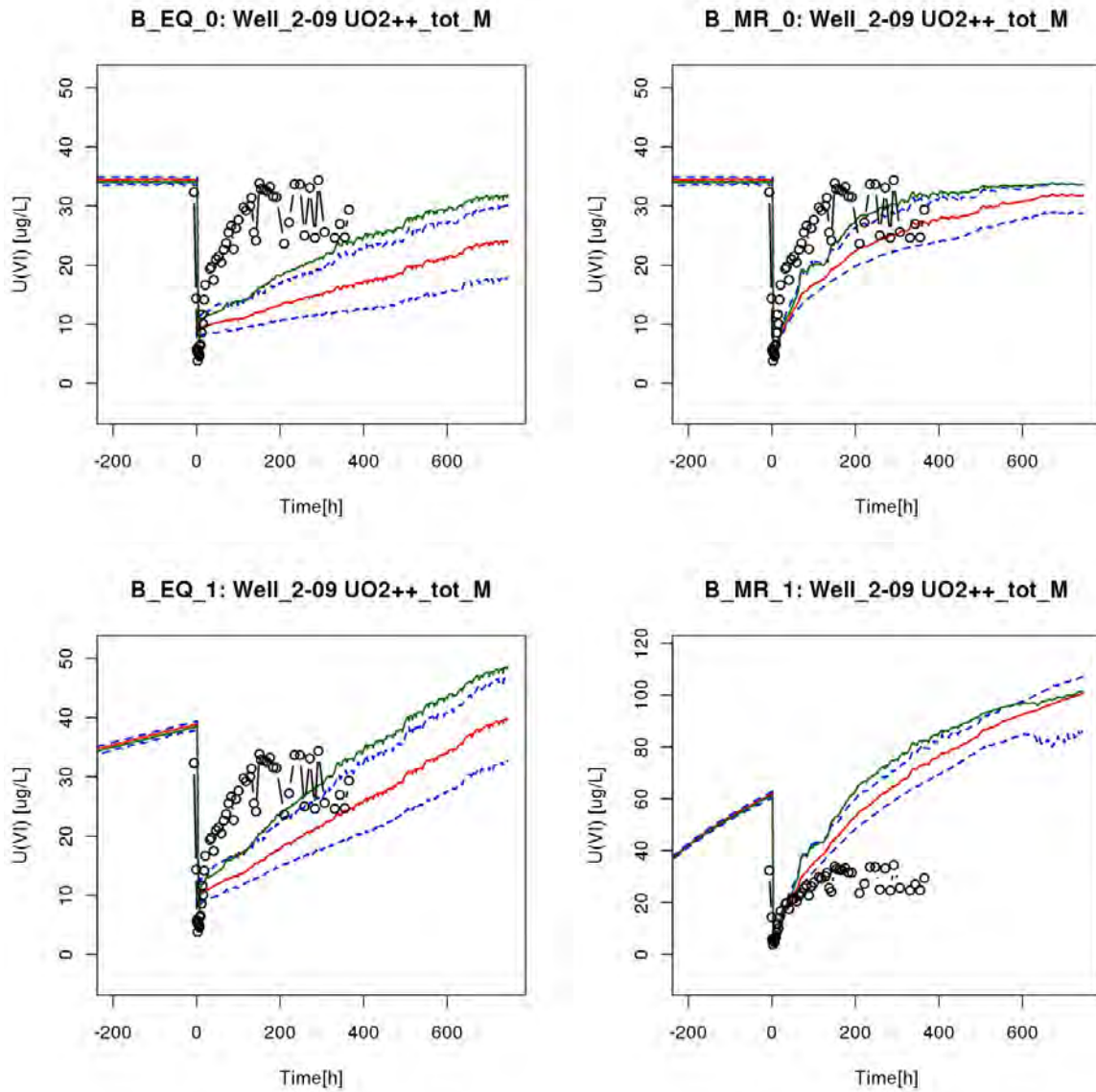


Figure 8: Comparison of model simulations for U(VI) concentration with field data for boundary condition scenario B.

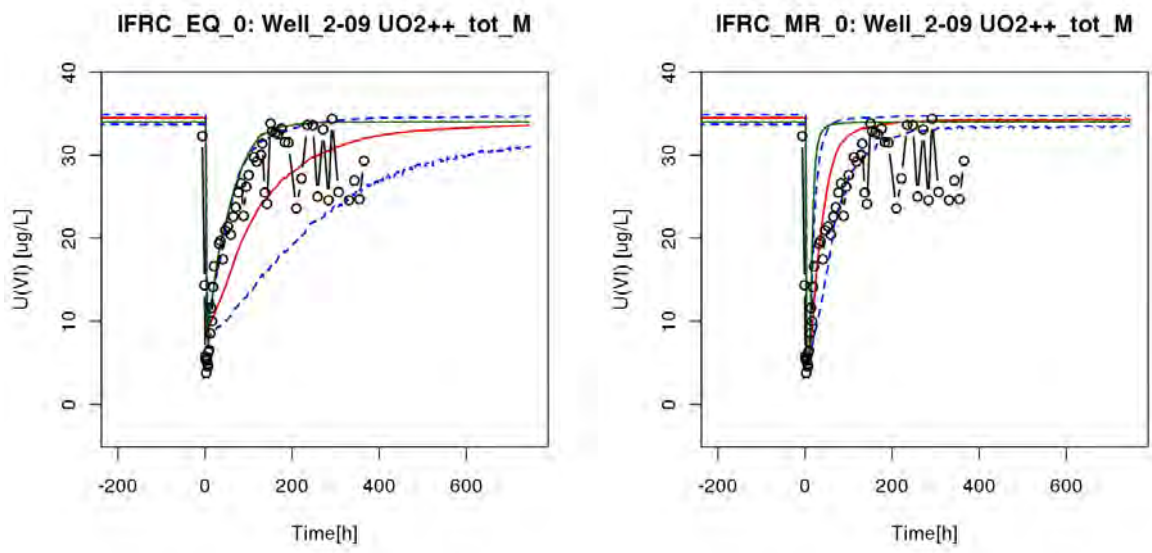


Figure 9: Comparison of model simulations for U(VI) concentration with field data for boundary condition scenario C.